Biochimica et Biophysica Acta, 1141 (1993) 29–36

BBABIO 43750

The computed free energy change of hydrolysis of inorganic pyrophosphate and ATP: apparent significance for inorganic-pyrophosphate-driven reactions of intermediary metabolism

Julia M. Davies [a,1], Ronald J. Poole [a] and Dale Sanders [b]

[a] *Department of Biology, McGill University, Montreal (Canada) and* [b] *Department of Biology, University of York, Heslington, York (UK)*

(Received 27 April 1992)
(Revised manuscript received 19 August 1992)

Key words: Free energy change; Inorganic pyrophosphate; Pyrophosphate; ATP; Thermodynamic model; Metabolism

Energy from cytosolic hydrolysis of inorganic pyrophosphate (PP_i) can be conserved through PP_i acting as a specific phosphoryl donor or through the substitution of reactions involving PP_i for those involving ATP. To assess the relative importance of PP_i in this context, the standard free energy change ($\Delta G^{o\prime}$) and hence the actual free energy change (ΔG) values for ATP and PP_i hydrolysis have been computed for a simple model cytosol. $\Delta G^{o\prime}_{ATP}$ and $\Delta G^{o\prime}_{PP_i}$ show dissimilar responses to pH and free Mg^{2+}, with implications for cell energetics during anaerobiosis. The impact of the estimates on possible in vivo function of two primary H^+-translocating phosphoanhydrolases (an ATPase and PPase) at the vacuolar membrane of higher plants is discussed.

Introduction

Inorganic pyrophosphate (PP_i) plays a key role in metabolism. As a product of biosynthesis, its cytosolic hydrolysis drives anabolic reactions to completion (by lowering cytosolic PP_i levels) and it was long held that the energy of that hydrolysis is not harnessed. It is recognised that PP_i could be a significant energy donor, in some cases replacing ATP [1–5]. An example is afforded by eucaryote glycolysis where, in the committed step, the ATP-dependent phosphofructokinase (ATP-PFK,EC 2.7.1.11) can be replaced by a PP_i-dependent enzyme (PP_i-PFP, EC 2.7.1.90) in the production of fructose 1,6-bisphosphate [6].

In higher plants (and bacteria), the energetics of PP_i hydrolysis assume special significance. The readily-reversible PP_i-PFP reaction may provide an adaptive pathway for glycolysis and gluconeogenesis in higher plant cells [7]. PP_i-PFP (rather than ATP-PFK) is activated by the regulatory metabolite fructose 2,6-bisphosphate (Fru(2,6)P_2)[8]. The latter, in turn, has a role in regulation of photosynthetic sucrose synthesis and its production may be inhibited by PP_i [5]. The regulation of plant cytosolic PP_i levels (which appear to be highly stabilised [9]) cannot be through soluble alkaline pyrophosphatases, since these enzymes appear to be restricted to plastids [10]. Instead, regulation is thought to be afforded by the enzymes which could utilise PP_i hydrolysis as an energy source, including PP_i-PFP, UDPGlc pyrophosphorylase and the H^+-pumping pyrophosphatase of the vacuolar membrane (H^+-PPase, EC 3.6.1.1) [4,5]. The H^+-PPase is one of two primary H^+ pumps residing at the vacuolar membrane, the other being an H^+-ATPase (EC 3.6.1.3) [4]. Both translocate H^+ into the vacuolar lumen, thus generating a H^+ electrochemical gradient which can drive secondary transport systems.

Correspondence to: D. Sanders, Department of Biology, University of York, York, YO1 5DD, UK.
[1] Present address: University of York, York, UK.

Abbreviations: ADP, adenosine 5′-diphosphate; ATP, adenosine 5′-triphosphate; ATP-PFK, ATP-dependent phosphofructokinase; F, Faraday constant; Fru(2,6)P_2, fructose 2,6-bisphosphate; $\Delta G^{o\prime}$, standard Gibbs free energy change; ΔG, actual Gibbs free energy change for given conditions; ΔH, enthalpy change; H^+-ATPase, H^+-pumping adenosine 5′-triphosphatase; H^+-PPase, vacuolar H^+-pumping inorganic pyrophosphatase; K_{eq}, equilibrium constant; K_{obs}, observed equilibrium constant; K_{ref}, reference equilibrium constant; $[K^+]_v$, vacuolar potassium activity; pH_c, cytosolic pH; P_i, inorganic orthophosphate; PP_i, inorganic pyrophosphate; PP_i-PFP, pyrophosphate:fructose-6-phosphate phosphotranferase; R, gas constant; T, temperature in kelvin; UDPGlc, uridine 5′-diphosphoglucose; γ, activity coefficient; $\Delta\Psi$, membrane potential difference; $[\ ]_f$, activity of free ion; $[\ ]_{total}$, total activity of ion.

The importance of PP_i in cellular energetics may be understood more fully by a consideration of its free energy of hydrolysis in cytoplasmic conditions (ΔG_{PP_i}). However, the restricted pH range and discrete Mg^{2+} levels deployed in previous in vitro studies to estimate $\Delta G^{\circ\prime}$ has limited the flexibility of such considerations. Moreover, it is necessary to consider concurrently the behaviour of ATP in individual systems, since both PP_i and ATP will bind ions from a common pool. It is such complexing of reactants and products which determines the equilibrium constant (K_{eq}), and therefore both $\Delta G^{\circ\prime}$ and ΔG. In this study we have attempted to improve modelling of cellular energetics by deriving $\Delta G^{\circ\prime}_{ATP}$, $\Delta G^{\circ\prime}_{PP_i}$ and hence ΔG_{ATP} and ΔG_{PP_i} values for feasible cytosolic conditions of PP_i, P_i (orthophosphate), ATP, ADP, Mg^{2+}, K^+, Ca^{2+} and pH. The model is based on a non-photosynthesising higher plant cell. The calculated $\Delta G^{\circ\prime}$ values are also presented as these may prove to be a useful resource for experimentation in which the use of non-physiological conditions is necessitated.

The $\Delta G^{\circ\prime}$ for hydrolysis of ATP and PP_i over a range of conditions can be derived from the K_{eq} for ATP and PP_i hydrolysis measured in fixed conditions, coupled with a knowledge of their respective ligand binding constants. From this it is possible to predict the in vivo poise of a range of ATP and PP_i-dependent enzymes (including the H^+ translocases of the plant vacuolar membrane) and hence assess their physiological significance. The vacuolar H^+-PPase is also modelled here as a H^+-K^+ symporter in light of its vectorial activation by K^+ at its cytosolic face [11] and the effect of K^+ on the reversal potential of the enzyme. Increasing extravacuolar K^+ concentration results in a positive shift in the reversal potential, which is in accord with the notion that the enzyme executes H^+-K^+ symport [12].

Materials and Methods

Derivation of a reference equilibrium constant (K_{ref}) for ATP hydrolysis at 37°C

K_{ref} for ATP hydrolysis was derived using the method described by Rosing and Slater [13]. This method involves the estimation of an equilibrium constant for a set reference reaction, free of metal ions. The K_{ref} then enables calculation of the apparent equilibrium constant of the overall hydrolysis reaction for any given condition of pH, free Mg^{2+}, free K^+ etc. The reference reaction was:

$$HATP^{3-} + H_2O \leftrightarrow HADP^{2-} + H_2PO_4^- \quad (1)$$

The mean equilibrium activities at 37°C of K, Mg, ATP, ADP and P_i in each of the five glutamine synthetase experiments listed in Table II of Ref. 13 were used to compute the equilibrium activities of the reference species in each case. Activities of complexes at equilibrium were computed for the given conditions of temperature, ionic strength and pH from the association constants of the reactants. Association constants were taken from Refs. 14–16. The complexes considered were: $KATP^{3-}$, $KADP^{2-}$, $KHPO_4^-$, KH_2PO_4, $MgATP^{2-}$, $MgHATP^-$, $MgADP^-$, MgHADP, $MgHPO_4$, $HATP^{3-}$, H_2ATP^{2-}, $HADP^{2-}$, H_2ADP^-, $H_2PO_4^-$ (designated Complex group A). A value of free Mg^{2+} ($[Mg^{2+}]_f$) activity at equilibrium was generated for each example. $[Mg^{2+}]_f$ was within 10% of the estimates given in Ref. 13. $[Mg^{2+}]_f$ was used to produce a K_{obs} for ATP hydrolysis using the equation provided in Ref. 13:

$$K_{obs} = 242.(\gamma\text{glutamine}/\gamma^2 NH_4\text{glutamate}) .(1 + 7.66[Mg^{2+}]_f).K_{a\,obs} \quad (2)$$

where γ is an activity coefficient and $K_{a\,obs}$ is the equilibrium constant for the glutamine synthetase reaction (these values are provided in Ref. 13 for each case). A K_{ref} value was obtained from each K_{obs} using the equation:

$$K_{ref} = \{(y.ADP \cdot y.P_i)/y.ATP\}.K_{obs} \quad (3)$$

where y.ADP, $y.P_i$ and y.ATP are the molar fractions $[HADP^{2-}]/[\Sigma ADP]$, $[H_2PO_4^-]/[\Sigma P_i]$ and $[HATP^{3-}]/[\Sigma ATP]$, respectively. Σ specifies the sum of the species present and [ ] specifies chemical activity. A mean K_{ref} of 5.69 $(\pm 0.36) \cdot 10^5$ M for ATP hydrolysis at 37°C was obtained. Apparent K_{ATP} values for any given set of ionic conditions at 37°C could be then obtained as:

$$K_{ATP} = \{y.ATP/(y.ADP \cdot y.P_i)\}.K_{ref} \quad (4)$$

The accuracy of the K_{ref} estimated was evaluated by using it to predict the K_{obs} for ATP hydrolysis for the experimental cases listed in Ref. 13. The accuracy of the predicted K_{obs} ranged from 82% to 127% with a mean of 100% ± 7% for the five cases sampled.

Adjusting the reference equilibrium constant for ATP hydrolysis at 25°C

A K_{ref} for 25°C was derived using the van't Hoff isochore and a mean enthalpy change (ΔH) for ATP hydrolysis at pH 8.0 (-19.86 kJ mol^{-1}) from Refs. 17,18). A ΔH_{ref} from the latter value was obtained thus [13]:

$$\Delta H_{ref} = -4.75 + \{(K_1/(H^+))/(1 + K_1/(H^+))\}.\Delta H_1 - \{(K_2/(H^+))/(1 + K_2/(H^+))\}.\Delta H_2 - \{(K_3/(H^+))/(1 + K_3/(H^+))\}.\Delta H3 \quad (5)$$

where K_1, K_2 and K_3 are the ionisation constants for $HATP^{3-}$, $HADP^{2-}$ and $H_2PO_4^-$ and ΔH_1, ΔH_2, ΔH_3 the enthalpy change for each ionisation, respectively (enthalpy data from Ref. 19). A ΔH_{ref} of -24.16 kJ mol^{-1} was calculated. From the equation:

$$\log K_{ref\,T2}/\log K_{ref\,T1} = (-\Delta H_{ref}/2.303.R).(T_1 - T_2/T_1.T_2) \quad (6)$$

where R has its usual meaning, T_1 and T_2 are 37°C and 25°C, respectively, K_{ref} at 25°C was calculated as $8.3 \cdot 10^5$ M.

Derivation of a reference equilibrium constant (K_{ref}) for PP_i hydrolysis

The reference reaction was:

$$HP_2O_7^{3-} + H_2O \leftrightarrow 2HPO_4^{2-} + H^+ \quad (7)$$

Equilibrium activities of the reference complexes were computed from the thermodynamic data of Ref. 20 obtained at 25°C (Table II, cases 12 and 13). Association constants were taken from Refs. 14–16. The complexes considered were: $KP_2O_7^{3-}$, $KHP_2O_7^{2-}$, $KHPO_4^-$, KH_2PO_4, $MgP_2O_7^{2-}$, $Mg_2P_2O_7$, $MgHP_2O_7^-$, $MgHPO_4$, $HP_2O_7^{3-}$, $H_2P_2O_7^{2-}$, $H_3P_2O_7^-$, $H_4P_2O_7$, $H_2PO_4^-$ (designated Complex group B). A K_{ref} for each case was calculated using the equation:

$$K_{ref} = \{(y.P_i)^2/y.PP_i\}.K_{obs} \quad (8)$$

where $(y.P_i)^2$ and $y.PP_i$ are the molar fractions $([HPO_4^{2-}]/\Sigma P_i])^2$ and $[HP_2O_7^{3-}]/[\Sigma PP_i]$, respectively. A mean K_{ref} of $7.77 \cdot 10^3$ M was obtained (upper value $8.66 \cdot 10^3$ M, lower value $6.88 \cdot 10^3$ M). Apparent K_{PP_i} for 25°C values could then be obtained using the equation:

$$K_{PP_i} = \{y.PP_i/(y.P_i)^2\}.K_{ref} \quad (9)$$

A K_{ref} for 37°C was derived using the van't Hoff isochore. ΔH for PP_i hydrolysis at pH 7.4 was -7.9 kJ mol^{-1} [20]; ΔH for the ionisation of $HP_2O_4^{3-}$ and HPO_4^{2-} were $+1.67$ kJ mol^{-1} [21] and -3.3 kJ mol^{-1} [22], respectively. ΔH_{ref} was -2.76 kJ mol^{-1} and from this K_{ref} at 37°C was $7.44 \cdot 10^3$ M.

Estimation of $\Delta G^{o\prime}$ and ΔG for ATP and PP_i hydrolysis in the model cytoplasm

The input parameters used to obtain estimates of K_{ATP} and K_{PP_i} were pH, K, Mg, Ca, ATP, ADP, PP_i and P_i. Unless otherwise stated, the following values were used and maintained in the simulation (in mM): $[K^+]_{total}$ 100 [23], $[Mg^{2+}]_f$ 0.4 [24], $[Ca^{2+}]_f$ 0.0002 [25], $[ATP]_{total}$ 2.3, $[ADP]_{total}$ 0.31, $[PP_i]_{total}$ 0.25 [10], $[P_i]_{total}$ 5 [25],(pH 7.3 [26]). The ATP and ADP values were derived from Ref. 27 by assuming a cytoplasmic volume of 15 and 20 μl/mg chlorophyll [28] and taking the mean (estimates are for non-photosynthesising cells). The complex species considered were groups A and B combined with the addition of: $CaATP^{2-}$, $CaHATP^-$, $CaADP^-$, CaHADP, $CaP_2O_7^{2-}$, $CaHP_2O_7^-$, $Ca_2P_2O_7$ [14–16]. Thus, a common pool of reactants and products existed in the simulations. Simulations were performed with temperature set at 25°C or 37°C. $\Delta G^{o\prime}$ values were calculated from:

$$\Delta G^{o\prime} = -RT \ln K_{eq} \quad (10)$$

ΔG values for ATP hydrolysis were calculated from:

$$\Delta G_{ATP} = \Delta G^{o\prime} + RT \ln\{([ADP]_{total} + [P_i]_{total})/[ATP]_{total}\} \quad (11)$$

ΔG values for PP_i hydrolysis were calculated from:

$$\Delta G_{PP_i} = \Delta G^{o\prime} + RT \ln\{[P_i]^2_{total}/[PP_i]_{total}\} \quad (12)$$

Energetics of the vacuolar H^+-ATPase and H^+-PPase

Values of K_{ATP} and K_{PP_i} obtained from the default conditions for the cytoplasm at 25°C were used to model the free energy relations of the enzymes. Pump action was described as [4]:

(a) H^+-ATPase;

$$nH_c^+ + ATP \leftrightarrow nH_v^+ + ADP + P_i \quad (13)$$

Thus,

$$\Delta G = nF\Delta\Psi - RT \ln\{(K_{ATP}.[ATP].[H^+]_c^n)/([ADP].[P_i].[H^+]_v^n)\} \quad (14)$$

(b) H^+-PPase;

$$nH_c^+ + PP_i \leftrightarrow nH_v^+ + 2P_i \quad (15)$$

Thus,

$$\Delta G = nF\Delta\Psi - RT \ln\{(K_{PP_i}.[PP_i].[H^+]_c^n)/([P_i]^2.[H^+]_v^n)\} \quad (16)$$

(c) H^+-PPase as a H^+-K^+ symporter;

$$nH_c^+ + mK_c^+ + PP_i \leftrightarrow nH_v^+ + mK_v^+ + 2P_i \quad (17)$$

Thus,

$$\Delta G = (n+m)F\Delta\Psi - RT \ln\{(K_{PP_i}.[PP_i].[H^+]_c^n.[K^+]_c^m)/([P_i]^2.[H^+]_v^n.[K^+]_v^m)\} \quad (18)$$

where subscripts c and v refer to cytoplasmic and vacuolar compartments, respectively, n and m are the stoichiometric ratios of H^+ and K^+ translocated per

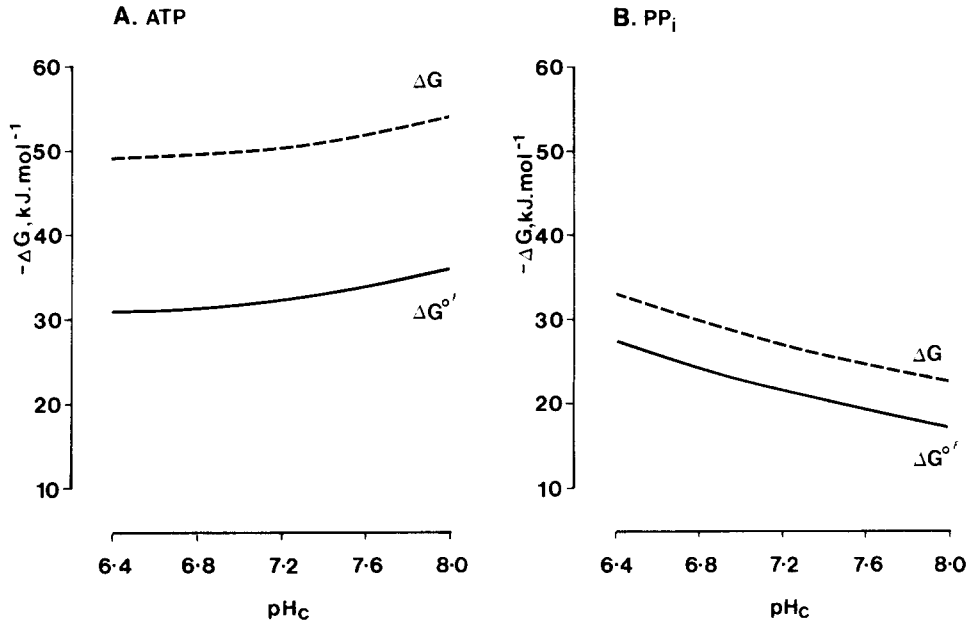

Fig. 1. The variation with model cytoplasmic pH (pH_c) of $\Delta G^{o\prime}$ and ΔG for ATP and PP_i hydrolysis. (a) ATP hydrolysis; $\Delta G^{o\prime}$ solid line, ΔG broken line. (b) PP_i hydrolysis; $\Delta G^{o\prime}$ solid line, ΔG broken line. $\Delta G^{o\prime}$ was estimated at 25°C with pH as a variable but with the remaining default conditions maintained (i.e., in mM:[ATP] = 2.3, [ADP] = 0.31, $[P_i] = 5$, $[PP_i] = 0.25$, $[K^+] = 100$, $[Mg^{2+}]_f = 0.4$, $[Ca^{2+}]_f = 0.0002$). ΔG_{ATP} and ΔG_{PP_i} were estimated using Eqns. 11 and 12, respectively, and the default values of reactants and products.

ATP or PP_i hydrolysed and $\Delta\Psi$ is the trans-tonoplast membrane potential difference. $\Delta\Psi$ was taken as +20 mV referenced to the cytoplasm [29].

Results

Evaluation of the estimation of cytoplasmic complexes

The computational procedure was tested using the cytoplasmic concentrations of ATP, ADP, P_i and free Mg^{2+} (0.82, 0.22, 4, 0.4 mM, respectively) estimated to be present at pH 7.3 in mung bean root tips by NMR spectroscopy (Ref. 24). $[K^+]_{total}$ and $[Ca^{2+}]_f$ were set at 100 mM and 200 nM, respectively. $[Mg]_{total}$ was set at 1.4 mM to generate $[Mg^{2+}]_f$ of 0.4 mM. Where Yazaki et al. estimated that > 90% of ATP is bound to Mg, we predicted 87%. Similarly, the in vivo ratio of $MgATP/ATP_{free}$ estimated in Ref. 24 at 9.45 was 10.62

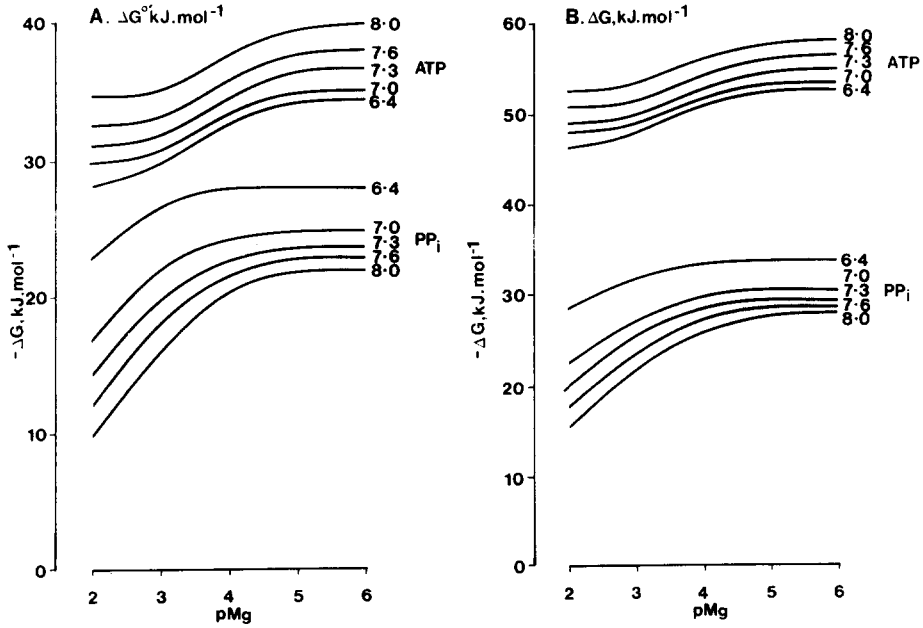

Fig. 2. The variation of $\Delta G^{o\prime}$ and ΔG for ATP and PP_i hydrolysis as a function of free Mg^{2+} (pMg) and model cytoplasmic pH. (a) $\Delta G^{o\prime}$. (b) ΔG. Estimates were produced for 25°C. Remaining default conditions were maintained as for Fig. 1.

in this study. To our knowledge, no comparable experimental work is available to afford a direct test of PP_i complex predictions.

$\Delta G^{\circ\prime}$ and ΔG for ATP and PP_i hydrolysis under model cytoplasmic conditions

Using the default conditions for estimation of $\Delta G^{\circ\prime}$ (see Materials and Methods) at 25°C, K_{ATP} was estimated to be $5.65 \cdot 10^5$ M ($\Delta G^{\circ\prime} = -32.8$ kJ mol^{-1}; $\Delta G = -50.9$ kJ mol^{-1}). The standard error of the K_{ref} for ATP, (K_{ATP} could range from $5.9 \cdot 10^5$ to $5.4 \cdot 10^5$ M) had little impact on $\Delta G^{\circ\prime}$ (-32.9 to -32.7 kJ mol^{-1}) or, accordingly, ΔG (-51.0 to -50.8 kJ mol^{-1}). K_{PP_i} was estimated as $6.04 \cdot 10^3$ M, ranging from $6.7 \cdot 10^3$ or $5.4 \cdot 10^3$ M if the upper or lower values of the K_{ref} for PP_i were used, respectively. The $\Delta G^{\circ\prime}$ for PP_i hydrolysis was thus -21.6 kJ mol^{-1} (upper value -21.8, lower -21.3) and ΔG was -27.3 kJ mol^{-1} (upper -27.5, lower -27.0). Fig. 1 illustrates the effect of varying cytoplasmic pH at 25°C (all other parameters constant). The values for 37°C differed by < 1.5 kJ mol^{-1} from those displayed. As predicted in Ref. 13, $\Delta G^{\circ\prime}_{ATP}$ becomes more positive with decreasing pH. Conversely, the negativity of $\Delta G^{\circ\prime}_{PP_i}$ increases dramatically as pH is lowered – a result which agrees qualitatively with that observed experimentally by De Meis [22]. The value of $\Delta G^{\circ\prime}_{PP_i}$ lies within 4 kJ mol^{-1} of $\Delta G^{\circ\prime}_{ATP}$ at low values of cytosolic pH ($pH_c = 6.4$). However, at pH_c 6.4 ΔG_{PP_i} (the actual energy change for the model cytosolic conditions) lies 16 kJ mol^{-1} more positive than ΔG_{ATP}. Clearly, at neutral pH_c ΔG_{ATP} is nearly twice that of ΔG_{PP_i}.

Values of $\Delta G^{\circ\prime}_{ATP}$ and $\Delta G^{\circ\prime}_{PP_i}$ over a cytosolic $[Mg^{2+}]_f$ range of 1 μM to 10 mM (pMg 2 to 6) at varying pH (6.4 to 8.0) are shown in Fig. 2a. The sigmoidal relationship for $\Delta G^{\circ\prime}_{ATP}$ shows both good qualitative and quantitative agreement with that described in Ref. 13. For example, at pH 7.0 and p*Mg* 3 $\Delta G^{\circ\prime}_{ATP}$ is -30 kJ mol^{-1} (cf. -28 kJ mol^{-1} [13]), at p*Mg* 6 it is -36 kJ mol^{-1} (cf. -34 kJ mol^{-1} [13]). The predicted $\Delta G^{\circ\prime}_{PP_i}$ values support the observations [22,30] that K_{PP_i} decreases with increasing Mg^{2+}. $[Ca^{2+}]_f$ had no discernible impact on either $\Delta G^{\circ\prime}_{ATP}$ or $\Delta G^{\circ\prime}_{PP_i}$ over the range 200 to 650 nM at pH 7.3, 25°C.

The predicted actual free energy changes (ΔG_{ATP} and ΔG_{PP_i}) for the model cytosol over a cytosolic $[Mg^{2+}]_f$ range of 1 μM to 10 mM at pH 6.4 to 8.0 are shown in Fig. 2b. The potential of PP_i as a phosphoryl donor is favoured by low $[Mg^{2+}]_f$ and low pH_c; at 1μM $[Mg^{2+}]_f$ (pMg 6) and pH_c 6.4, PP_i hydrolysis in the model cytosol would release 65% of the energy available from ATP hydrolysis. Increasing $[P_i]$ to 15 mM at 25°C had insignificant effect on $\Delta G^{\circ\prime}$ values for both ATP and PP_i hydrolysis at pH_c 7.0; ΔG_{ATP} became less negative by 3 kJ mol^{-1} and ΔG_{PP_i} became less negative by 5 kJ mol^{-1}.

Anaerobiosis was simulated by decreasing ATP arbitrarily to 0.5 mM and increasing ADP to 2.11 mM at pH 7.3, 6.8, 6.4, 6.0 at 25°C (Simulation A). Thus the [ATP]/[ADP] ratio decreased from the default value of 7.42 to 0.24. Total PP_i was held at 0.25 mM as it is independent of the [ATP]/[ADP] ratio [31]. Table I shows both the $\Delta G^{\circ\prime}$ and ΔG values for ATP and PP_i hydrolysis at default and anaerobiotic nucleotide ratios. At each pH considered, the calculated $\Delta G^{\circ\prime}_{ATP}$ and $\Delta G^{\circ\prime}_{PP_i}$ values remained as for the default [ATP]/[ADP] ratio of 7.42 at that pH. Through Eqn. 11, ΔG_{ATP} for the 0.24 [ATP]/[ADP] ratio becomes 8.5 kJ mol^{-1} less negative than the default value at each pH. As PP_i was independent of the nucleotide ratio, ΔG_{PP_i} values remained unchanged. At pH 7.3, ΔG_{PP_i} is 15 kJ mol^{-1} more positive than ΔG_{ATP} but at pH 6.0 it is only 5 kJ mol^{-1} more positive.

To maintain $[Mg^{2+}]_f$ and $[Ca^{2+}]_f$ at 0.4 mM and 200 nM (respectively) during simulation, total levels of the ions were adjusted accordingly. However, if it were assumed that under respiratory inhibition, $[Mg^{2+}]_f$ and $[Ca^{2+}]_f$ could not be maintained at their homeostatic levels then it becomes reasonable to run the anaerobiosis simulation without those adjustments to $[Mg^{2+}]_{total}$

TABLE I

$\Delta G^{\circ\prime}$ and ΔG values for ATP and PP_i hydrolysis obtained for control and simulated anaerobiotic conditions

For the control, the default conditions (an [ATP]/[ADP] ratio of 7.42) were used. For simulated anaerobiosis, an [ATP]/[ADP] ratio of 0.24 was used but $[PP_i]$ and $[P_i]$ retained their default values. pH_c varied for both cases. $[Mg^{2+}]_{total}$ was adjusted to maintain $[Mg^{2+}]_f$ at 0.4 mM and $[Ca^{2+}]_{total}$ was adjusted to maintain $[Ca^{2+}]_f$ at 200 nM. Estimates were made at 25°C.

pH:	7.3		6.8		6.4		6.0	
[ATP]/[ADP]:	7.42	0.24	7.42	0.24	7.42	0.24	7.42	0.24
$[Mg^{2+}]_{total}$ (mM):	2.75	1.8	2.55	1.75	2.50	1.4	2.15	1.2
$[Mg^{2+}]_f$ (mM):	0.4	0.4	0.4	0.4	0.4	0.4	0.4	0.4
$\Delta G^{\circ\prime}_{ATP}$ (kJ mol^{-1})	−32.8	−32.8	−31.4	−31.4	−31.2	−31.2	−31.1	−31.1
ΔG_{ATP} (kJ mol^{-1})	−50.9	−42.4	−49.5	−41.0	−49.3	−40.8	−49.2	−40.7
$\Delta G^{\circ\prime}_{PP_i}$ (kJ mol^{-1})	−21.6	−21.6	−24.6	−24.6	−27.4	−27.4	−30.1	−30.1
ΔG_{PP_i} (kJ mol^{-1})	−27.3	−27.3	−30.3	−30.3	−33.1	−33.1	−35.8	−35.8

TABLE II

$\Delta G^{\circ\prime}$ and ΔG values for ATP and PP_i hydrolysis for simulated anerobiotic conditions (Simulation B)

An [ATP]/[ADP] ratio of 0.24 was used but [PP_i] and [P_i] retained their default values. $[Mg^{2+}]_{total}$ was fixed at the default value of 2.75 mM and $[Ca^{2+}]_{total}$ was fixed at the default value of 680 nM.

pH:	7.3	6.8	6.4	6.0
$[Mg^{2+}]_{total}$ (mM):	2.75	2.75	2.75	2.75
$[Mg^{2+}]_f$ (mM):	0.7	0.9	1.1	1.4
$\Delta G^{\circ\prime}_{ATP}$ (kJ mol^{-1})	−31.1	−29.5	−29.0	−29.0
ΔG_{ATP} (kJ mol^{-1})	−40.7	−39.2	−38.6	−38.6
$\Delta G^{\circ\prime}_{PP_i}$ (kJ mol^{-1})	−19.8	−23.0	−26.0	−29.2
ΔG_{PP_i} (kJ mol^{-1})	−25.5	−28.7	−31.7	−34.9

and $[Ca^{2+}]_{total}$. Hence, $\Delta G^{\circ\prime}_{PP_i}$, $\Delta G^{\circ\prime}_{ATP}$, ΔG_{PP_i} and ΔG_{ATP} were calculated for the [ATP]/[ADP] ratio of 0.24 at pH 7.3, 6.8, 6.4 and 6.0, but $[Mg^{2+}]_{total}$ and $[Ca^{2+}]_{total}$ were maintained at 2.75 mM and 680 nM, respectively (Simulation B). These were their values for the default conditions at pH 7.3. The results of this simulation method are shown in Table II. $\Delta G^{\circ\prime}_{PP_i}$ became slightly more positive than its default value at each pH. At pH 7.3, ΔG_{PP_i} is 15 kJ mol^{-1} more positive than ΔG_{ATP} but at pH 6.0 it is only 4 kJ mol^{-1} more positive. At the pH values considered, when $[Mg^{2+}]_{total}$ and $[Ca^{2+}]_{total}$ were held constant the $[Mg^{2+}]_f$ value under simulated anaerobiosis was always higher than the 0.4 mM default value. A comparison may be made with the study of Yazaki et al. [24], where a 10 min exposure to 10 mM sodium azide induced an increase in $[Mg^{2+}]_f$ from 0.4 to 0.68 mM (the ATP/ADP ratio fell from 3.79 to 0.37). When only $[Mg^{2+}]_{total}$ was held constant but $[Ca^{2+}]_{total}$ varied to keep $[Ca^{2+}]_f$ at 200 nM, the $\Delta G^{\circ\prime}$ (and hence ΔG) values were the same as those obtained when both total ion activities were held constant. Overall, it is clear that, regardless of the simulation method used, the values of $\Delta G^{\circ\prime}_{PP_i}$ and ΔG_{PP_i} move closer to those of $\Delta G^{\circ\prime}_{ATP}$ and ΔG_{ATP}, respectively, with decreasing pH_c.

Energetics and poise of the vacuolar H^+-ATPase and H^+-PPase

Fig. 3a illustrates the free energy changes of the H^+-ATPase ($n = 1$, 2 or 3) modelled with the default parameters (pH_c 7.3 etc.), K_{ATP} $5.65 \cdot 10^5$ M and using Eqn. 14. The $n = 2$ relationship is also shown for [P_i] set at 15 mM [32]. K_{ATP} becomes $5.79 \cdot 10^5$ M in this case. Fig. 3b presents the predicted ΔG values for the H^+-PPase modelled with the default values and using Eqn. 16 for the enzyme as a H^+-pump with a stoichiometric ratio (n) of 1 or 2 $H^+ : PP_i$ or Eqn. 18 for the enzyme as a H^+-K^+ symporter. In the latter case, the stoichiometric ratios were $n{:}m = 1:1$ or $1:2$ and vacuolar K^+ (K^+_v) was set at 200 mM [23]. The ΔG for the $n = 2$ H^+-pump has also been calculated with [P_i] = 15 mM. The impact of P_i on ΔG for the H^+ – PPase is not significantly greater than on ΔG for the H^+-ATPase, despite its more pronounced relevance through Eqns. 16 and 18. Analysis of enzyme substrate concentrations, showed that neither pump would be limited kinetically over the pH range 7 to 8. MgATP increased from 1.97 to 2.03 mM ($K_m = 0.6$ mM [33]). $MgPP_i$ (which is widely held to be the substrate of the H^+-PPase) increased from 72 to 186 μM (K_m = 15–20 μM [33]). Mg_2PP_i (which may be the true substrate – Leigh, Pope, Jennings and Sanders, submitted) increased from 7 to 16 μM.

Discussion

The validity of the K_{ATP}, K_{PP_i}, $\Delta G^{\circ\prime}$ and ΔG predictions rest on the choice of vital components in the model, the quality of the data available to quantitate them and the level of understanding of their interactions and interdependence. The paucity of information on cytoplasmic levels of the reactants and their complexes (particularly of Mg) limits further verification of our estimates. In the absence of a body of in vivo data describing the interaction of the chosen components, the assumption made for computation (that all but the

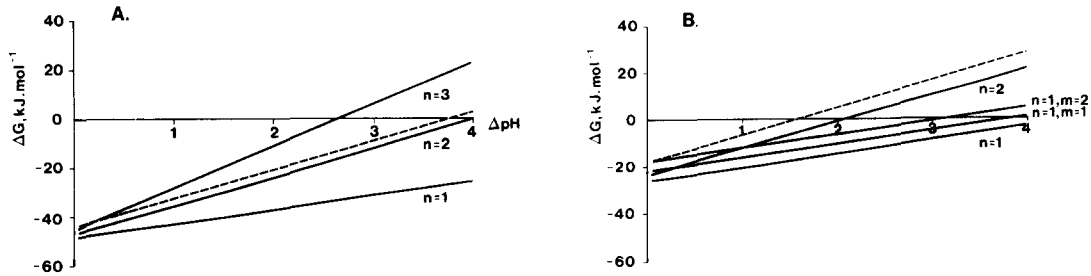

Fig. 3. The tonoplast H^+-ATPase and H^+-PPase ΔG estimates under default conditions (25°C) and with $\Delta\Psi$ set at +20 mV. (a) The H^+-ATPase modelled for stoichiometric ratios $n = 1$, 2 or 3, using Eqn. 14. The dotted line is for $n = 2$ but with [P_i] = 15 mM and $K_{ATP} = 5.79 \cdot 10^5$ M. (b) The H^+-PPase modelled for $n = 1$ or 2 (Eqn. 16) and as a H^+-K^+ symporter with a $H^+ : K^+$ stoichiometry ($n:m$) of 1:1 or 1:2 (Eqn. 18). $[K^+]_v$ was set at 200 mM [23]. The dotted line is for the $n = 2$ H^+-pump with [P_i] = 15 mM ($K_{PP_i} = 6.9 \cdot 10^3$ M).

variable parameter remain constant in the simulation) is crude but unavoidable.

Given these caveats, it is clear that $\Delta G^{\circ\prime}_{ATP}$, ΔG_{ATP}, $\Delta G^{\circ\prime}_{PP_i}$ and ΔG_{PP_i} differ markedly as a function of pH and free Mg^{2+}. At normal values of cytoplasmic pH (7.2–7.3) ATP would still have the greater potential as a phosphoryl donor. The potential for PP_i to substitute for ATP is favoured by low pH and low free Mg^+. The impact of the HPO_4^{2-} complex on the $\Delta G^{\circ\prime}_{PP_i}$ calculation becomes more pronounced at lower pH; at pH 8 it accounts for 70% of total P_i, at pH 6.4 only 20%.

That the ΔG_{PP_i} values estimated for anaerobic conditions did not differ from the control whilst ΔG_{ATP} values became more positive (when $[Mg^{2+}]_f$ and $[Ca^{2+}]_f$ were held constant; Simulation A) suggests that both acidosis and reduced ATP availability would favour substitution of PP_i for ATP in these conditions. The pattern of increasing negativity of ΔG_{PP_i} with decreasing pH can be seen from the alternative simulation where $[Mg^{2+}]_{total}$ and $[Ca^{2+}]_{total}$ were held constant (and free ion activity varied; Simulation B).

Higher plant tissues may survive for over 18 h under anaerobic conditions and glycolysis proceeds for most of this time [34,35]. Anaerobiosis induces a 0.4 to 0.8 unit decrease in plant cytosolic pH [26]. This would partly be the result of inhibition of the ATP-dependent plasmamembrane and tonoplast H^+ pumps. In maize root tips, cytosolic pH decreases by 0.5 units within 20 min of exposure to anoxia and remains stable [36]. Cytosolic PP_i levels are known to remain constant during prolonged periods of anoxia whereas those of ATP (in the same tissue) fall drastically [37]. The stability of cytosolic PP_i, even under conditions where its biosynthetic production would be inhibited, suggests that this homeostasis is of great importance to the cell. The near parity of ΔG_{ATP} and ΔG_{PP_i} at low pH and $[Mg^{2+}]_f$ indicates that PP_i energisation of reactions limited by the restricted availability of ATP may be feasible, although it is clear from Fig. 2 and Tables I and II that such a conclusion rests on cytosolic levels of $[Mg^{2+}]_f$. While it is thought that it is the ability of higher plants to switch to ethanolic fermentation [36] (and so operate an effective cytosolic "pH stat" [38,39]) which enables them to endure prolonged anoxia, the relatively increased energy available from PP_i at lowered pH may also be an important factor in maintaining critical cell functions.

In the context of energisation of H^+ transport into the higher plant vacuole, the few available measurements of tonoplast membrane potential have necessitated some generalisation in the calculation of ΔG for the in vivo action of the tonoplast H^+-ATPase and H^+– PPase. The predictions reaffirm the observation that stoichiometry is a critical determinant of physiological poise [4]. The H^+-ATPase measured stoichiometry of 2 [40] fits the model of a strongly hydrolytic pump, operable at physiological pH and capable of pumping H^+ into the lumen against a pH gradient of up to 4 units.

The H^+-PPase would also be poised as an inwardly-directed pump if its stoichiometry were unity. If greater, it could be regarded as a regulator of cytosolic PP_i and P_i, under the control of the gradients established by the H^+-ATPase. When the H^+-PPase is modelled as a K^+-H^+ symporter, it is then capable of being hydrolytically poised and pumping both H^+ and K^+ against a ΔpH of 3 to 4 units and again this argument is contingent on an $H^+ : PP_i$ stoichiometry of 1. As such the PPase could facilitate vacuolar K^+ accumulation [23].

Overall, development of predictive in vivo models for bioenergetics may assist in the understanding of physiological function and regulation. Although the model presented here is of a non-photosynthesising plant cell, it could readily be extended to encompass cytoplasmic conditions during photosynthesis. Of the input parameters employed, only $[Ca^{2+}]_f$ undergoes a profound and stable change on a dark to light transition. For plant cells, the role of PP_i in carbon flow, pH regulation and transport merits further attention in relation to its in vivo energetic potential.

Acknowledgements

The authors are grateful to the Agricultural and Food Research Council, U.K. (Grant PG87/501) and the Natural Science and Engineering Research Council (Canada) for financial support. D.S. was a Science Research Fellow of the Nuffield Foundation, whose support is also acknowledged. We are indebted to Dr. D.C.S. White for provision of software enabling calculation of ligand-ion complexes.

References

1 Baltscheffsky, H., Von Stendigk, L.-V., Heldt, H.-W. and Klingenberg, M. (1966) Science 153, 1120–1121.
2 Baltscheffsky, M. (1967) Nature 216, 241–243.
3 Wood, H.G. (1977) Fed. Proc. 9, 2197–2205.
4 Rea, P.A. and Sanders, D. (1987) Physiol. Plant. 71, 131–141.
5 Stitt, M. (1990) Annu. Rev. Plant Physiol. Plant Mol. Biol. 41, 153–185.
6 Mertens, E. (1991) FEBS Lett. 285, 1–5.
7 Black, C.C., Mustardy, L., Suna, S.S., Kormanik, P.P., Xu, D.-P. and Paz, N. (1987) Physiol. Plant. 69, 387–394.
8 Sabularse, D.C. and Anderson, R.L. (1981) Biochem. Biophys. Res. Commun. 103, 848–854.
9 Quick, P., Neuhaus, E., Feil, R. and Stitt, M. (1989) Biochim. Biophys. Acta 973, 263–271.
10 Weiner, H., Stitt, M. and Heldt, H.W. (1987) Biochim. Biophys. Acta 893, 13–21.
11 Davies, J.M., Rea, P.A. and Sanders, D. (1991) FEBS Lett. 278, 66–68.
12 Davies, J.M., Poole, R.J., Rea, P.A. and Sanders, D. (1992) Proc. Natl. Acad. Sci. USA, in press.

13 Rosing, J. and Slater, E.C. (1972) Biochim. Biophys. Acta 267, 275–290.
14 Smith, R.M. and Martell, A.E. (1975) Critical Stability Constants, Vol.2, pp. 281–283, Plenum, New York.
15 Smith, R.M. and Martell, A.E. (1976) Critical Stability Constants, Vol. 4, pp. 56–59, Plenum, New York.
16 Martell, A.E. and Smith, R.M. (1982) Critical Stability Constants, Vol. 5, pp. 260–261 & 407–408, Plenum, New York.
17 Kitzinger, C. and Benzinger, T. (1955) Z. Naturforsch. 10, 375–381.
18 Podolsky, R.J. and Morales, M.F. (1956) J. Biol. Chem. 218, 945–959.
19 Phillips, R.C., George, P. and Rutman, R.J. (1963) Biochemistry USA 2, 501–508.
20 Flodgaard, H. and Fleron, P. (1974) J. Biol. Chem. 249, 3465–3474.
21 Irani, R.R. and Taulli, T.A. (1966) J. Inorg. Nucl. Chem. 28, 1011–1020.
22 De Meis, L. (1984) J. Biol. Chem. 259, 6090–6097.
23 Leigh, R.A. and Wyn Jones, R.G. (1984) New Phytol. 97, 1–14.
24 Yazaki, Y., Asukagawa, N., Ishikawa, Y., Ohta, E. and Sakata, M. (1988) Plant Cell Physiol. 29, 919–924.
25 Rebeille, F., Bligny, R. and Douce, R. (1984) Plant Physiol. 74, 355–359.
26 Kurkdjian, A. and Guern, J. (1989) Annu. Rev. Plant Physiol. Plant Mol. Biol. 40, 271–303.
27 Stitt, M., Lilley, R.McC. and Heldt, H.W. (1982) Plant Physiol. 70, 971–977.
28 Gerhardt,R. and Heldt, H.W. (1984) Plant Physiol. 75, 542–547.
29 Spanswick, R.M. and Williams, E.J. (1964) J. Exp. Bot. 15, 193–200.
30 Daley, L.A., Renosto, F. and Segel, I.H. (1986) Anal. Biochem. 157, 385–395.
31 Dancer, J., Veith, R., Fell, R., Komor, E. and Stitt, M. (1990) Plant Sci. 66, 59–63.
32 Stitt, M., Wirtz, W., Gerhardt, R., Heldt, H.W., Spencer, C. and Walker, D.A. (1985) Planta 166, 354–364.
33 Hedrich, R., Kurkdjian, A., Guern, J. and Flugge, U.I. (1989) EMBO J. 8, 2835–2841.
34 Sachs, M.M., Freeling, M. and Okimoto, R. (1980) Cell 20, 761–768.
35 Neal, M.J. and Girton, R.E. (1955) Am. J. Bot. 42, 733–737.
36 Roberts, J.K.M., Callis, J., Wemmer, D., Walbot, V. and Jardetsky, O. (1984) Proc. Natl. Acad. Sci. USA 81, 3379–3383.
37 Dancer, J.E. and ap Rees, T. (1989) Planta 178, 421–424.
38 Davies, D.D. (1973) Symp. Soc. Exp. Biol. 27, 513–529.
39 Smith, F.A. and Raven, J.A. (1979) Annu. Rev. Plant Physiol. 30, 289–311.
40 Bennett, A.B. and Spanswick, R.M. (1984) Plant Physiol. 74, 545–548.